Intelligent Optimal Dispatching of Multi-Energy Microgrid Based on Improved Ant Colony Algorithm

Anqi Xu, Siquan Li, Xu Guo, Wenlong Ji, Yanling Shang, and Fangzheng Gao

***Abstract*—To address the issues of slow convergence and local optima in traditional microgrid scheduling, an optimization strategy for multi-energy microgrid scheduling based on an improved ant colony algorithm (ACA) is proposed to enhance the accuracy, stability, and convergence speed of microgrids. Firstly, mathematical models for power generation units such as wind, photovoltaic, fuel cell, and energy storage are constructed with their influencing factors analyzed. Subsequently, constraint conditions including power balance and energy storage state are established. An improved ant colony algorithm incorporating regulation factor decay, Boltzmann selection strategy, and deflection angle correction is designed. Finally, case analysis is conducted to compare the microgrid under islanded conditions, which validates that the improved ant colony algorithm in this paper can effectively reduce costs and possesses good economic efficiency and environmental sustainability.**

***Index Terms*—multi-energy, islanded microgrid, improved ant colony algorithm, optimal scheduling**

I. INTRODUCTION

With the continuous growth of global energy demands, traditional fossil fuel resources are gradually being depleted and environmental pollution problems are becoming increasingly severe [1]. The power grid is currently facing unprecedented challenges. Traditional power grids, which rely on large-scale centralized power generation and long-distance power transmission, are not only energy-inefficient but also vulnerable to natural disasters and equipment failures, resulting in insufficient power supply reliability [2]. Moreover, the rapid development of clean energy, such as wind energy and solar energy, has further increased the complexity and uncertainty of power grid operation due to the instability and intermittency of their output [3].

Before the emergence of microgrids, the power grid system mainly relied on centralized power generation and transmission and distribution networks. Although this model has ensured large-scale power supply over the past few decades, it has also brought about numerous problems, such as energy waste, high transmission losses, serious environmental pollution and a strong dependence on a single power source. Especially in the areas with high penetration rates of wind and solar energy as well as in remote areas, it is difficult for traditional power grids to provide a stable and reliable power supply, which has affected local economic development and the quality of life of residents.

As an innovative power system, microgrids consist of distributed generation (DG), energy storage devices and loads, which can flexibly operate in both grid-connected and off-grid modes [4]. A microgrid can not only effectively absorb and utilize clean energy such as wind energy and solar energy, but also smooth energy fluctuations through the energy storage system to provide a stable and reliable power supply [5]. The advantages of microgrids are as follows: Improved energy utilization efficiency: Through local power generation and local consumption, transmission losses are reduced and energy utilization efficiency is enhanced. Enhancing power supply reliability: When disconnected from the main grid, the microgrid can operate independently to ensure the stable power supply for critical loads. Reducing environmental pollution: By utilizing clean energy and improving energy efficiency, the emissions of greenhouse gases and other pollutants are decreased. Flexibility and scalability: Microgrids can flexibly adjust their scales and configurations according to requirements to adapt to different application scenarios and load demands [6].

At present, many scholars have conducted relevant research on the optimal scheduling of microgrids. Most of them use intelligent optimization algorithms to solve the problems. In [7], the linear differential decreasing weight was proposed and the mutation strategy was introduced to improve the multi-objective particle swarm optimization algorithm, so as to reduce the optimization cost of microgrids. In [8], a multi-objective microgrid optimal scheduling strategy based on the improved bird swarm algorithm was put forward, which improved the accuracy, stability and

Manuscript received April 8, 2025; revised July 7, 2025. This work was partially supported by the National Natural Science Foundation of China under grant 61873120, the National Natural Science Foundation of Jiangsu Province under grants BK20201469 and BE2021016-5, and the Qing Lan project of Jiangsu Province.

Anqi Xu is a postgraduate student in the School of Automation, Nanjing Institute of Technology, Nanjing 211167, China (email: njit_airobot@126.com).

Siquan Li is a postgraduate student in the School of Automation, Nanjing Institute of Technology, Nanjing 211167, China (email: y00450230122@njit.edu.cn).

Xu Guo is a postgraduate student in the School of Automation, Nanjing Institute of Technology, Nanjing 211167, China (email: y00450240314@njit.edu.cn).

Wenlong Ji is a postgraduate student in the School of Automation, Nanjing Institute of Technology, Nanjing 211167, China (email: y00450240413@njit.edu.cn).

Yanling Shang is an associate professor in the School of Automation, Nanjing Institute of Technology, Nanjing 211167, China (corresponding author, e-mail: hnnhsyl@126.com).

Fangzheng Gao is a professor in the School of Automation, Nanjing Institute of Technology, Nanjing 211167, China (e-mail: gaofz@126.com).

convergence degree of multi-objective optimization of microgrids. In [9], an optimization method based on the adaptive ACA was proposed, which effectively reduced the operating cost and environmental pollution of the microgrid system and ensured the power supply stability. In [10], a variable universe hybrid FFOPID controller was proposed to improve the frequency control performance of islanded microgrids. In [11], an optimal configuration method based on the improved adaptive noise complete ensemble empirical mode decomposition was proposed to solve the problem of tie-line power fluctuations caused by the fluctuations of renewable energy output and electricity load in grid-connected microgrids. In [12], a multi-strategy improved whale optimization algorithm was proposed to address the optimal dispatching problem of regional interconnection multi-microgrids. In [13], a disturbance rejection controller for power quality enhancement in microgrids was proposed, which employed the walrus optimization algorithm to determine optimal gains for the Fractional Order ADRC and a multi - functional recurrent fuzzy neural network for adaptive control parameter prediction, effectively improving power quality under grid disturbances. In [14], an improved bald eagle search algorithm (IBES) based on fusion opposition-based learning and Cauchy mutation was proposed, which achieved higher accuracy and effectively reduced the economic cost of the microgrid group system. In [15], a cuckoo search algorithm with inter-dimensional reverse perturbation learning based on compound chaotic mapping was proposed, which effectively improved the total daily operation benefit and system operation stability of microgrids. In [16], an improved grey wolf optimizer (IGWO) was proposed to solve the transferable load model in the microgrid scheduling model. In [17], an improved hybrid crow search algorithm (IHCSA) was proposed to solve the multi-objective optimal power flow (MOOPF) problem. In [18], an enhanced sparrow search algorithm (ESSA) was proposed to optimize the economic dispatch (ED) in isolated microgrids.

This paper will mainly focus on the optimal scheduling of microgrids in the islanded state. An optimal scheduling model of microgrids composed of wind power, photovoltaic power, gas turbines and energy storage will be established. The mathematical models of each unit will be introduced in detail, and different constraint conditions will be set up to analyze the power consumption of important loads in microgrids under the islanded state. The improved ant colony algorithm will be applied to solve the mathematical models in microgrids, determine the output of each unit, so as to achieve the lowest total cost. Moreover, the feasibility of the algorithm proposed in this paper will be verified through case analysis.

II. The Model Of Microgrids Power Generation Units

In this section, the mathematical description of optimal scheduling model of microgrids is introduced.

A. WT Model

The output characteristics of wind power generators are shown in Equation (1).

$$\mathbf{P}_{WT}=\begin{cases}0 & v<v_{ci}\\ k_2\cdot v^2+k_1\cdot v+k_0 & v_{ci}<v<v_{\gamma}\\ P_t & v\le v\le v_{co}\\ 0 & v>v_{co}\end{cases} \tag{1}$$

where k_0 , k_1 , k_2 are the operating characteristic parameters of the wind power generation motor; v_{ci} is the cut-in wind speed, v_r the rated wind speed, v_o is the cut-out wind speed, and P_t is the rated value of the output power of the generator.

Although wind power systems have high installation costs, their operational costs are low. Additionally, they are environmentally friendly, producing almost no greenhouse gas emissions. In view of these factors, the power generation amount of wind turbine units should be increased as much as possible in the economic dispatch of microgrids.

B. PV Model

The open-circuit voltage of a solar cell is related to light intensity and temperature. An increase in light intensity and a decrease in temperature will lead to an increase in the open-circuit voltage; the short-circuit current increases with the increase in light intensity and temperature. The output power of a solar cell is closely related to light intensity and temperature: the output power increases when the light intensity becomes stronger, while it decreases when the temperature rises. Since the temperature coefficient of a solar cell is negative, an increase in temperature will result in a decline in its output power and efficiency. The power output model of a solar power generation system is expressed as shown in Equation (2).

$$\mathrm{P}_{PV}=\mathrm{P}_{STC}\frac{G_{ING}}{G_{STC}}[1+k(T_C-T_r)] \tag{2}$$

where $\mathrm{P_{PV}}$ is the output power (kW) when the light intensity is $\mathrm{G_{ING}}$ (W/m²); $\mathrm{P_{STC}}$ is the maximum output power (kW) of the solar power generation system under standard conditions ($\mathrm{G_{SNG}}$ = 1000 W/m² and T = 25°C); k is the power temperature coefficient; T_C is the temperature of the solar cell; T_r is the reference temperature.

The output characteristics of solar cells are affected by light intensity and temperature, which makes it difficult to accurately predict their output power. As a result, they cannot be freely dispatched in the microgrid system and belong to the non-adjustable units. In order to balance the power generation and electricity demand, a battery bank can be configured in the solar power generation system, and the regulation ability of the system can be improved through a bidirectional converter.

C. MT Model

The mathematical model expression of the micro gas turbine when it serves as a combined heat and power generation unit is shown as follows:

$$Q_{MT}=\frac{P_e(1-\eta_e-\eta_l)}{\eta_e} \tag{3}$$

$$Q_{CO}=Q_{MT}\times COP_{CO} \tag{4}$$

$$Q_{he}=Q_{MT}\times COP_{he} \tag{5}$$

$$V_{MT} = \frac{\sum P_e \cdot \Delta t}{\eta_e \cdot LHV_f} \quad (6)$$

where η_e is the power generation efficiency of the micro gas turbine; η_l is the heat loss coefficient when the micro gas turbine is working. In Equation (5), Q_{he} is the heating capacity supplied by the micro gas turbine to the load; Q_{CO} is the cooling capacity supplied to the load; COP_{CO} and COP_{he} are the cooling coefficient and heating coefficient of the lithium bromide chiller respectively; Δt is the operating time of the micro gas turbine; V_{MT} is the volume of natural gas consumed by the micro gas turbine in the time period (m³); LHV_f is the lower heating value of natural gas (kW·h/m³), with a value of 9.7 kW·h/m³.

The mathematical expression for the total efficiency of the micro gas turbine during operation is shown in Equation (7).

$$\eta = \frac{P_e + Q_{MT}}{m_f LHV} \quad (7)$$

where P_e represents the active power supplied when the micro gas turbine operates normally (kW); Q_{MT} is the recovered thermal power of the gas turbine (kW); LHV is the low heating value of natural gas (kWh/m³); m_f is the flow rate of the fuel (m³/h).

The mathematical expression for the fuel cost when the micro gas turbine generates electricity is shown in Equation (8).

$$C_{MT} = C_{nl} \frac{1}{LHV} \sum \frac{P_J}{\eta_J} \quad (8)$$

where C_{nl} is the local natural gas price (yuan/m³); LHV is the low heating value of natural gas (kWh/m³); P_J is the output power of the micro gas turbine within the time interval J (kW); η_J is the working efficiency of the micro gas turbine within the interval J.

D.Fuel Cell Model

The mathematical model of a fuel cell includes the cost of power generation and the working efficiency. The magnitude of the working efficiency of a fuel cell mainly depends on the active power output of the cell (P_{FC}), and its efficiency (η_{FC}) is shown in Equation (9).

$$\eta_{FC} = -0.0024 P_{FC} + 0.6735 \quad (9)$$

The calculation expression for the power generation cost of the fuel cell is shown in Formula 10.

$$C_{FC} = C_{nl} \frac{1}{LHV} \sum_J \frac{P_J}{\eta_J} \quad (10)$$

where C_{nl} represents the price of local natural gas (yuan/m³); LHV is the low heating value of natural gas (kWh/m³); P_J is the active power provided by the fuel cell within time J (kW); η_J is the overall efficiency of the cell within time J.

E. ESS Model

In a microgrid, renewable energy sources such as wind power and solar power generation are easily affected by factors like wind speed, temperature, and light intensity, which are characterized by randomness and volatility. This leads to instability in the grid voltage and frequency and makes it difficult to adapt to load changes in a timely manner. Energy storage devices can enhance the security, flexibility, and reliability of the microgrid by performing peak shaving and valley filling through rapid response. During the peak power generation period, the energy storage devices store the surplus electric energy; when there is insufficient power generation, they can quickly provide the stored electric energy to ensure the balance between supply and demand as well as voltage stability. The specific parameters of the storage battery are described as follows:

(1) Battery Capacity of the Storage Battery

The battery capacity of a battery refers to all the electric energy that can be discharged under specific discharge conditions. The magnitude of the battery capacity is represented by C, and the unit is A.

(2) State of Charge (SOC) of the Storage Battery in the Energy Storage Device

The State of Charge (SOC) of the storage battery in the energy storage device refers to the ratio of the current capacity (C_r) in the storage battery to the rated capacity (C_n) of the storage battery. Its calculation model is shown in Equation (11).

$$SOC = (C_r / C_n) \times 100\% \quad (11)$$

When the charge and discharge efficiency of the storage battery is the highest, the SOC of the storage battery is within the range of 60% - 80%. According to the operation strategy of the microgrid it should be made to work within this range as much as possible.

(3) Depth of Discharge (DOD) of the Storage Battery

The Depth of Discharge (DOD) of the storage battery refers to the percentage of the total amount of electricity currently discharged (Q_-) during its discharge process to the rated capacity (C_N). The calculation model is shown in Equation (12).

$$DOD = Q_- / C_N \quad (12)$$

(4) Depth of Charge (DOC) of the Storage Battery

The Depth of Charge (DOC) of the storage battery refers to the percentage of the amount of electricity provided by the external circuit (Q_+) during the charging process by the outside world to its own rated capacity (C_N). The calculation model is shown in Equation (13).

$$DOC = Q_+ / C_N \quad (13)$$

(5) Service Life of the Storage Battery

The Cycle Life of the storage battery refers to the cumulative number of charge and discharge cycles when its actual capacity drops to a certain value. Experiments show that the service life is closely related to the depth of discharge. The higher the depth of discharge, the more serious the life loss. The energy storage device model adopted in this paper mainly considers its storage capacity constraints and charge and discharge power constraints. The mathematical model expressions of the energy storage device are shown in Equations (14) and (15).

$$I_e = \frac{P_{bat}(t)}{U} \quad (14)$$

$$SOC(\mathrm{t})=\begin{cases} SOC(t-1)+\dfrac{\eta_{ch}\times I_e(t)}{C_N} & \text{charge} \\ SOC(t-1)-\dfrac{I_e(t)}{C_N\times\eta_{dis}} & \text{discharge} \end{cases} \quad (15)$$

where $I_{\mathrm{e}}(\mathrm{t})$ represents the actual charge and discharge current (at time t; $P_{bat}(t)$ represents the total power provided by the energy storage device up to time (kW); U represents the voltage value across the energy storage device (V). In Formula 15, $SOC(\mathrm{t})$ and $SOC(t-1)$ represent the State of Charge values of the energy storage device at time t and $(t-1)$ respectively; η_{ch} and η_{dis} represent the charge and discharge efficiency values of the energy storage device up to time t (%) respectively.

Before use, the working parameters of the energy storage device should be considered first, its State of Charge should be predicted, and the charge and discharge power and the number of charge and discharge cycles of the energy storage device should be constrained so that the service life of the energy storage device can be extended.

III. Objective Function And Constraint Equations For Optimal Dispatch Of Microgids

Toachieve the optimal operation of each unit and guarantee the lowest system operation cost of the microgrid, it is necessary to impose constraints on each power generation unit as:

(1) Power Balance Constraint:

$$P_d^t+P_{loss}^t=\sum_{i=1}^{N}P_{Gi}^t+P_{grid}^t \quad (16)$$

In the formula, P_d^t is the system load power within the time period t; P_{loss}^t is the power loss of the system transmission line within the time period t; P_{Gi}^t is the active power of each distributed generation unit within the time period t; P_{grid}^t is the active power traded between the main grid and the microgrid within the time period t.

(2) Power Constraint of the Output of Each Distributed Generation Unit:

$$\mathrm{P_i^{min}}\le \mathrm{P}_{Gi}\le \mathrm{P_i^{max}} \quad (17)$$

In the formula, $\mathrm{P_i^{min}}$ is the minimum active power provided by the micro power source i at time t; $\mathrm{P_i^{max}}$ is the maximum active power provided by the micro power source i at time t.

(3) Exchange Power Constraint between the Main Grid and the Microgrid:

$$P_{grid}^{\min}\le P_{grid\_i}\le P_{grid}^{\max} \quad (18)$$

where $P_{grid}^{\min}$ is the minimum value of the exchange power between the microgrid and the main grid; $P_{grid}^{\max}$ is the maximum value of the exchange power between the microgrid and the main grid.

(4) Power Constraint of the Energy Storage Unit:

$$P_{bt}^{\min}\le P_{bt}^i\le P_{bt}^{\max} \quad (19)$$

$$\sum_{i=1}^{T}P_{bt}^i\delta=0 \quad (20)$$

In the formula, $P_{bt}^{\min}$ is the maximum value of the charge and discharge power of the energy storage device; $P_{bt}^{\max}$ is the minimum value of the charge and discharge power of the energy storage device; δ is the scheduling time period.

IV. Optimal Operation Of Microgrids Based On The Improved Ant Colony Algorithm

A. Standard ACO Algorithm

The ant colony algorithm is a simulated evolutionary algorithm, which was initially used to solve the traveling salesman problem. The basic steps of the ant colony algorithm consist of two steps, namely the state transition probability and the pheromone update. The transition probability calculation formula for ant k to move from the current node i to the next node j at time t is as follows:

$$p_{ij}(t)=\begin{cases} \dfrac{\tau_{ij}^{\alpha}(t)\eta_{ij}^{\beta}(t)}{\sum_{s\in allowed}\tau_{ij}^{\alpha}(t)\eta_{ij}^{\beta}(t)} & (s\in allowed(k)) \\ 0 & (s\notin allowed(k)) \end{cases} \quad (21)$$

Among them $\eta_{ij}=1/d_{ij}$; $d_{ij}=\sqrt{(x_i-x_j)^2+(y_i-y_j)^2}$.

In the formula, α is the pheromone weight coefficient; β is the heuristic function weight coefficient; s is the number of visited cities; $\tau_{ii}(k)$ is the pheromone concentration function; $allowed(k)$ is the set of next feasible nodes; $n_{ii}(t)$ is the distance heuristic function; (x_i,y_i) is the coordinate of the current node; (x_j,y_j) is the coordinate of the next node j; d_{ii} is the distance between the current node i and the next node j; α is the pheromone heuristic factor; β is the expected heuristic factor.

After an ant completes a path search, under the action of the evaporation coefficient $\rho\,(0<\rho<1)$, the residual pheromone concentration in the previous iteration on this path evaporates, and the ants in the current iteration leave a new pheromone increment. The pheromone update mechanism is as follows:

$$\boldsymbol{\tau}_{ij}(t+1)=(1-\boldsymbol{\rho})\,\boldsymbol{\tau}_{ij}(t)+\Delta\boldsymbol{\tau}_{ij}(t) \quad (22)$$

where $\Delta\tau_{ij}(t)=\sum_{k=1}^{m}\Delta\tau_{ij}^k(t)$.

In the formula, Q is the pheromone intensity coefficient; L_k is the length of the path traveled by ant k in this round of iteration; m is the total number of ants in each round; $\Delta\tau_{ii}^k(t)$ is the pheromone generated by ant k on the path during this round of iteration (i,j); $\Delta\tau_{ii}(k)$ is the sum of the pheromones generated by all ants on the path in this round of iteration (i,j).

For the power grid system in this paper, if the traditional ant colony algorithm is used for micro-grid scheduling, there will be some deficiencies. For example, the convergence speed is slow, it is easy to fall into local optimal solutions. If the parameters are not set properly, it will also affect the algorithm effect. The computational complexity is high and the dynamic adaptability is poor. Therefore, an improved strategy is introduced for optimization.

B. Improved Ant Colony Algorithm

The fundamental ant colony algorithm suffers from the problems of a relatively small solution space due to the

scarcity of initial pheromone and a tendency of convergent to a local optimum during the algorithm operation. Therefore, a decay parameter for the adjustment factor, the Boltzmann selection strategy, the deflection angle factor, and the inflection point parameter are introduced in this paper to optimize the ant colony algorithm and improve its performance.

(1) Improvement of the Adjustment Factor Value

In the ant colony algorithm, α and β denote the respective influence coefficients of the pheromone τ_{ij} and the heuristic information η_{ij}. The value of α typically hovers around 1, whereas the value range of β is relatively wide. An excessively large β value makes the algorithm susceptible to getting stuck in a local optimum; conversely, an overly small β value leads to slow convergence of the algorithm. To prevent such situations, this paper introduces a decay parameter into β:

$$\beta=\begin{cases}\beta_0,\ 0<t\le 20\%\times t_{\max}\\ \sqrt{\beta_0\beta_1}^{(t/10)}\cdot\beta,\ 20\%\times t_{\max}<t\le 40\%\times t_{\max}\\ \beta_1,\ 40\%\times t_{\max}<t\le t_{\max}\end{cases}\quad(23)$$

where t is the number of iterations; $t_{\max}$ is the maximum number of iterations; β_0 and β_1 are constants, and $\beta_1>\beta_0$.

Equation (23) indicates that during the initial phase of the algorithm, a relatively small β value is set. This effectively maintains solution diversity in the initial search phase. In the intermediate phase of the algorithm, a decay strategy is implemented with a restricted number of decay instances. As a result, β can fluctuate within an effective interval, and the randomness of solutions is enhanced. In the final phase of the algorithm, a large β value is employed, which accelerates the algorithm's convergence and facilitates the search for the global optimum.

(2) Improved Pheromone Update Method

This paper borrows the Boltzmann selection mechanism to conduct further selection of the computed probability and randomly determine the subsequent path, so as to increase the search range of the ant colony, expand the solution space, and facilitate jumping out of the local optimum, as shown in Equations (24) and (25).

$$P_{ij}=\begin{cases}\dfrac{\exp\left[\dfrac{\tau_{ij}^{\alpha}(t)\eta_{ij}^{\beta}}{T}\right]}{\sum_{s\in D_k}\exp\left[\dfrac{\tau_{ij}^{\alpha}(t)\eta_{ij}^{\beta}}{T}\right]},\ j\in D_k\\ 0,\ j\notin D_k\end{cases}\quad(24)$$

$$T=T_0(0.99^{N-1})\quad(25)$$

where D_k is the feasible region; T is the temperature; N is the number of cycles.

The global pheromone updating approach is also refined. In the initial N_1 iterations, the ants that rank among the top G in the solution space release pheromone. After N_1 iterations, the global optimal solution is utilized for pheromone updating. To avoid the algorithm converging to a local optimum, during the intermediate phase of the algorithm's solution process, the traditional updating method is still employed for global pheromone updating, which are given in equations (26) and (27).

$$\tau_{ij}=\begin{cases}(1-\rho)\tau_{ij}+\rho\dfrac{\sum_{k\in BG}\Delta\tau_{ij}^{k}\xi_{ij}(t)^{\gamma}}{Z_{BG}\xi_{ij}(t)^{\gamma}},\ 0<N\le N_1\\ (1-\rho)\tau_{ij}+\rho\dfrac{\sum_{k\in Z_M}\Delta\tau_{ij}^{k}\xi_{ij}(t)^{\gamma}}{Z_{M}\xi_{ij}(t)^{\gamma}},\ N_1<N\le N_{\max}\end{cases}\quad(26)$$

$$BG=\left\{k\,|J_k(x)\le J_G(x),k\in(1,m)\right\}\quad(27)$$

where ρ is the pheromone evaporation factor; Z_{BG} is the number of ants in the set BG that choose the branch L_{ii}; Z_m is the number of all ants that choose the branch L_{ii}; γ is the direction deflection factor; $J_k(x)$ is the path function value of ant k; $J_G(x)$ is the path function value of the ant; m is the total number of ants.

Finally, with the aim of constraining the branch - selection angle and curtailing the frequency of branch deflections, thereby bringing the final path of the solution nearer to the true optimal path, this paper introduces the deflection angle factor θ_{ii} and the inflection point parameter G_k into the ant colony pheromone update formula, as demonstrated in equations (28) and (29).

$$\Delta\tau_{ij}^{k}=\begin{cases}\dfrac{Q}{J_x(x)+\varphi G_k},\ \textit{If ant k is on the path ij}\\ 0,\qquad\qquad\text{Otherwise}\end{cases}\quad(28)$$

$$\xi_{ij}=1-\frac{\theta_{ij}}{180}\quad(29)$$

where θ_{ii} represents the smaller angle between the direction vector of the previous branch and that of branch L_{ii}. When L_{ii} serves as the starting branch, $\theta_{ii}=0$, and θ_{ii} is expressed in degrees; G_k is the inflection point parameter of the path searched by the ant k; φ is the weighting coefficient; Q is a constant.

Equations (26) and (27) demonstrate that during the initial phase of the algorithm, the global pheromone update is executed by the ants ranked relatively high in the solution space releasing pheromone. By applying the improved β in Equation (23) to Equation (24), the problem that the algorithm falls into a local optimum in the solution stage is avoided to a large extent. Until after the iteration N_1, in order to further boost the accuracy and operation speed, all ants are used to release pheromone for global pheromone update. The convergence of the algorithm can be expedited by adjusting β_1.

C. Flowchart of Ant Colony Algorithm

(1) Initialization

Define the problem dimension, that is, the number of decision variables (including gas turbine power, fuel cell power, shedable load, and battery power); Initialize the pheromone matrix, with the initial pheromone value of each path being the same; Randomly generate a group of ants, where each ant represents a possible solution.

(2) Solution Construction

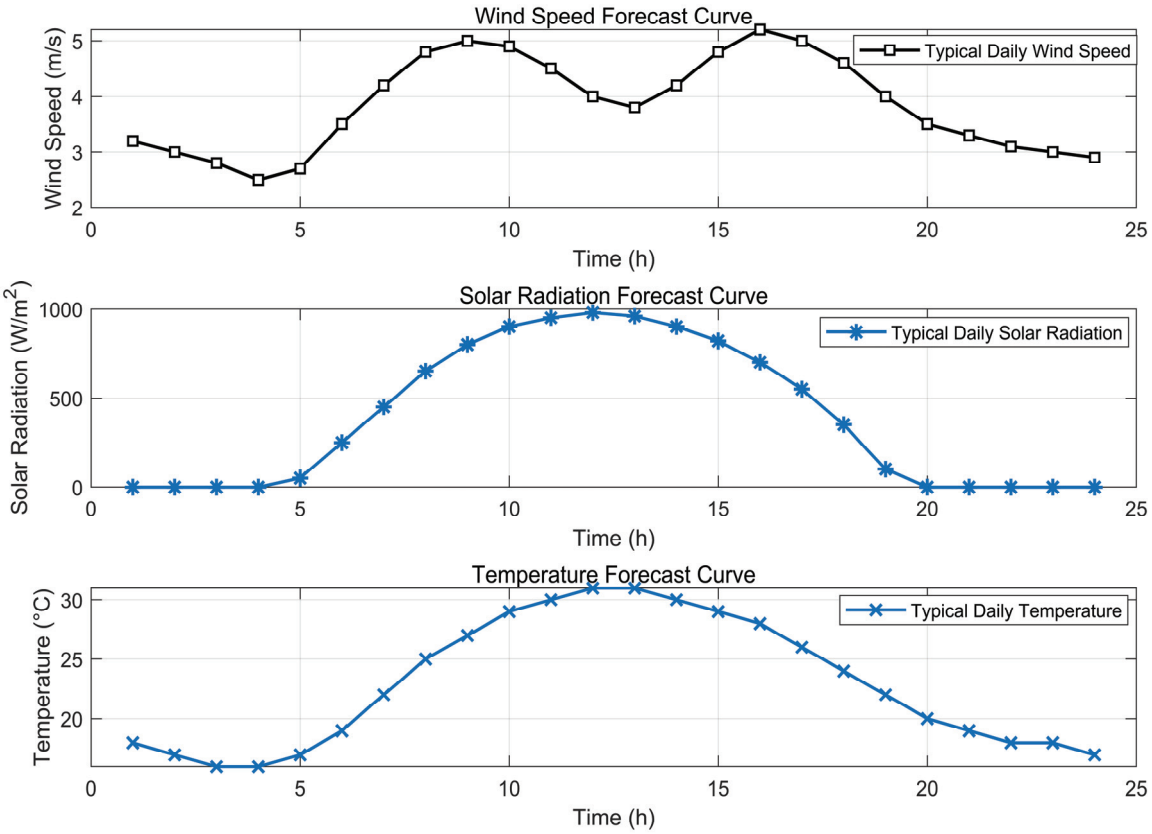

Fig. 1. Prediction curves.

Each ant computes transition probabilities based on pheromone concentration and heuristic information to select decision variable values. The search space is expanded through dynamic adjustment of heuristic function parameters combined with a Boltzmann selection strategy.

(3) Fitness Evaluation

Evaluate the fitness value of each ant's solution, that is, calculate the objective function value (such as the total operation cost); Record the path of each ant and the corresponding fitness value.

(4) Pheromone Update

Existing pheromone concentrations are first decayed according to the evaporation coefficient. Subsequently, high-quality paths are reinforced through pheromone intensification proportional to the fitness of the ant-generated solutions. The update process is further refined by incorporating a deflection angle factor and inflection point parameters to mitigate redundant path formation.

(5) Check the Termination Conditions

Verify if maximum iterations or preset fitness targets are met.

(6) Output Results

Output the best solution, that is, the decision variables (gas turbine power, fuel cell power, shedable load, and battery power) for each period; Calculate and output the hourly operation cost and other performance indicators.

V. .Case Study Analysis

A. Microgrid System Composition Model and Parameters

To verify the feasibility of the improved ant colony algorithm-based optimal scheduling strategy for islanded microgrids proposed in this paper, a typical regional one-day load curve and resource prediction data are selected as the basis for the case study. A microgrid model is constructed, which includes wind power, photovoltaic (PV) systems, gas turbines, fuel cells, energy storage devices, and shedable loads.

It can be seen from Fig. 1 that from 5:00 to 11:00, the light intensity gradually increases, so the output power of the power generation unit gradually increases. From 11:00 to 13:00, the light intensity is the strongest during the day, so the output power is the largest. From 13:00 to 19:00, the light intensity and the power generation power gradually decrease. From 19:00 to 5:00 the next day, the sunlight is zero, so the output of solar power generation is zero.

B. Simulation Analysis during Islanded Operation

This experiment uses MATLAB 2022 to analyze the microgrid model and utilizes the improved ant colony algorithm to solve the optimal scheduling of the microgrid for the established model. In this paper, one day is taken as a cycle for microgrid scheduling, and an hour is taken as a small optimal scheduling period to determine the scheduling of the distributed units of the microgrid and to determine the output cooperation of each unit. The parameter settings of the improved ant colony algorithm in this paper are as follows: the number of ant colonies is 120; the heuristic function factor is initially set to 4, and an attenuation mechanism is introduced to enhance search adaptability; the pheromone factor is 1; the volatility coefficient factor is 0.85; and the number of iterations is 150. The algorithm combines the Boltzmann selection strategy with the deflection angle constraint to improve path quality and avoid local optimality.

During a power grid failure or intentional islanding, the microgrid disconnects from the main grid and forms an independent small grid. It relies on local distributed generation equipment and energy storage devices to maintain power supply. The islanding operation mode needs to possess independence, self-regulation, and security to ensure power quality.

Since wind power generation and photovoltaic power generation are affected by wind speed and light intensity and are renewable energy sources, wind and solar power generation are preferentially used in microgrids. When wind and solar power generation cannot meet the electricity demand, the improved ant colony algorithm will be used to calculate the power supply from other power generation units to the system.

By leveraging the pre-established wind and solar power generation models and integrating parameters such as the actual wind speed, light intensity, and temperature on that day, their actual active power output is calculated. When the total output power of all generation units and energy storage devices in the microgrid fails to meet the load demand, the power supply to non-critical loads is temporarily suspended to ensure power balance between the system and the load, thus enabling the safe, stable, and economical operation of the microgrid system. Fig. 2 illustrates the output power of the wind and solar power generation units on a typical day.

It can be seen from the figure that solar power generation and wind power generation change with the changes in light and wind speed. From 6:00 to 19:00, the solar power generation power changes with the intensity of light. From 0:00 to 6:00 and from 19:00 to 24:00, the light intensity is zero, so the power generation power is also zero. Wind power output is distributed throughout the day with fluctuating patterns, reaching local peaks during early morning and late-night hours (e.g., 3:00 and 24:00). It remains relatively stable during the daytime, with the lowest valleys occurring around 9:00 and 20:00, approximately 15 kW. Overall, it demonstrates regulatory flexibility and auxiliary functionality.

When the microgrid is operating in an isolated state and the power generated by wind and solar energy falls short of meeting the load demand, taking the maximization of the total operating benefit of the microgrid as the objective function, use the improved ant colony algorithm to solve each constraint model and determine the output power of each unit. The power output situation is shown in Fig 3.

Micro Turbine (MT) plays a pivotal role in the islanded mode of microgrids, primarily tasked with delivering stable power output. During the early morning hours (0:00–6:00), due to the low load demand, MT operates at a reduced output level, only maintaining basic power supply to optimize fuel consumption and minimize operational costs. As the morning peak (6:00–10:00) arrives and electricity demand surges, MT gradually increases its power output to meet the rising load.

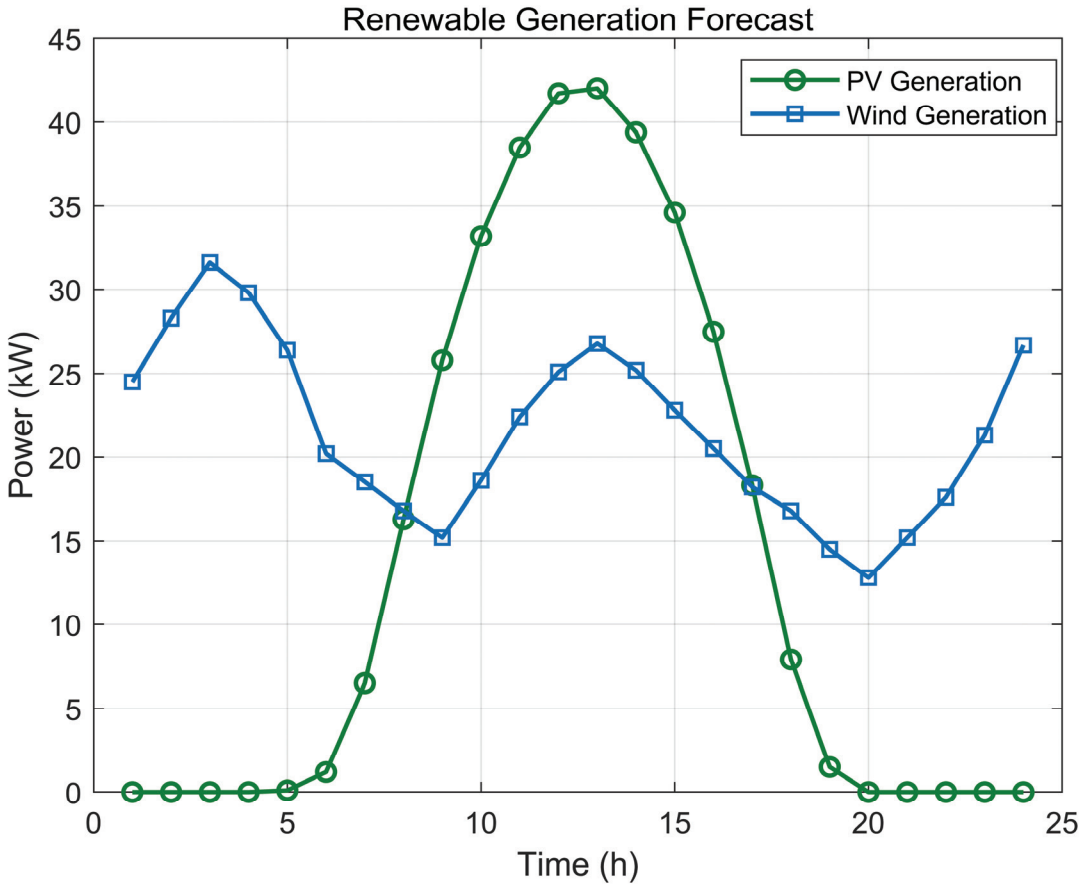

Fig. 2. Wind and solar power generation curves.

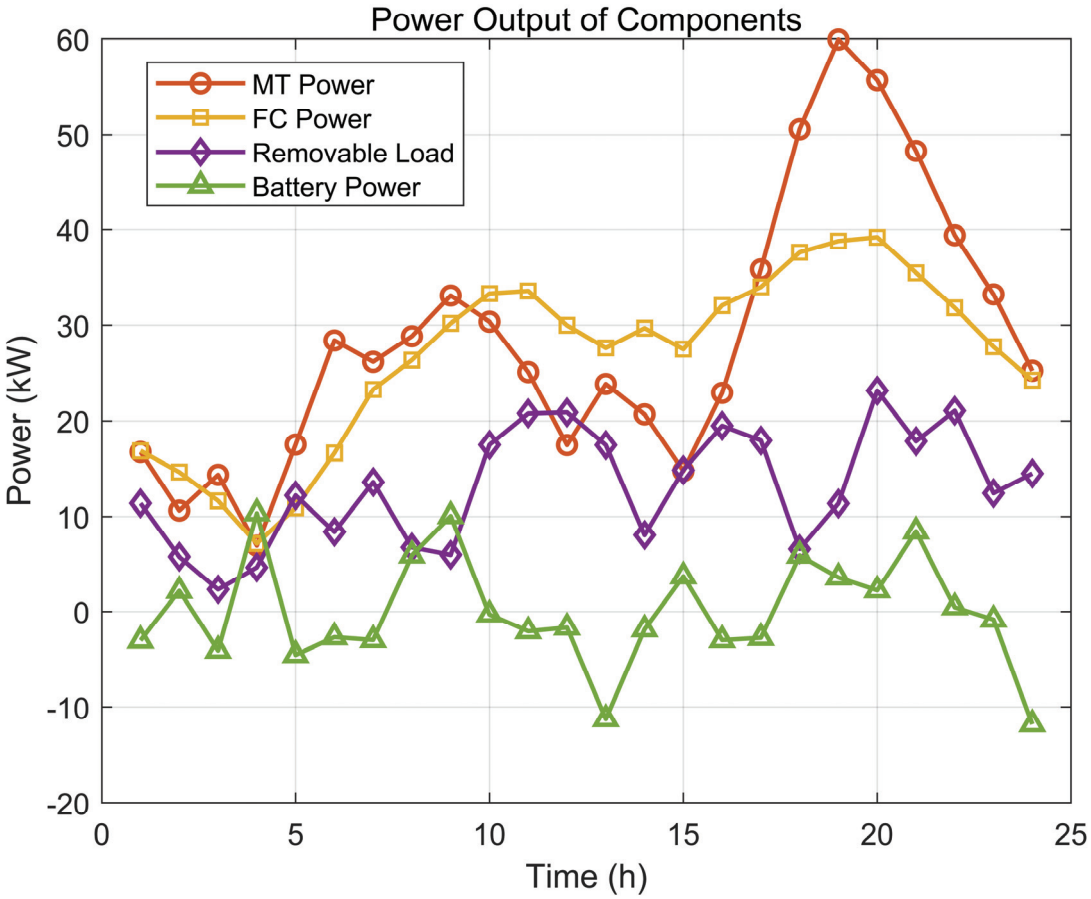

Fig. 3. Output diagram.

Throughout the daytime (10:00–18:00), MT maintains a relatively high output to provide essential power support for industrial and commercial activities. During the evening peak (18:00–22:00), driven by increased household electricity demand, MT's output reaches its daily maximum. At night (22:00–24:00), as load declines, MT scales back its output to low-level operation. Its flexible ramping capability enables rapid adjustment of power output to adapt to instantaneous load fluctuations, ensuring grid stability through precise power regulation algorithms.

Fuel Cell (FC) serves as an efficient and low-emission power source in islanded microgrids. In the early morning (0:00–6:00), FC operates at a low output to maintain base load, functioning efficiently under low-load conditions with minimal environmental impact. As the morning peak (6:00–10:00) emerges, FC gradually increases its output to assist in meeting peak demand and alleviate pressure on MT. During the daytime (10:00–18:00), FC maintains a stable medium-level output to supplement MT's power generation, ensuring consistent supply. During the evening peak (18:00–22:00), FC ramps up its output again to collaborate with MT in addressing high-load demands. At night (22:00–24:00), as demand wanes, FC reverts to base-load operation. The high efficiency and low-emission characteristics of FC make it invaluable in microgrids with strict environmental requirements, aligning with green energy optimization strategies.

Sheddable Load (X) plays a critical role in load management for islanded microgrids, allowing temporary curtailment of non-critical loads to safeguard essential services. During the early morning (0:00–6:00), with ample power supply, Px remains near zero, requiring no load shedding. As the morning peak (6:00–10:00) progresses and load increases, Px rises gradually, indicating the disconnection of non-critical loads to relieve grid stress. Throughout the daytime (10:00–18:00), with stable demand, Px stays low, with only minor load shedding during supply tightness. During the evening peak (18:00–22:00), significant load growth triggers a sharp increase in Px, leading to the curtailment of more non-critical loads to ensure grid stability. At night (22:00–24:00), as load decreases, Px diminishes, and power supply returns to normal. Effective management of sheddable loads smooths the load curve, enhancing microgrid flexibility and emergency response capabilities through prioritization and dynamic adjustment strategies.

The Battery Storage (BT) system is central to balancing power supply and demand in microgrids through energy storage and release. During the early morning (0:00–6:00), BT charges using surplus power from low-load nighttime periods, storing energy for future use. As the morning peak (6:00–10:00) begins, BT discharges to support peak demand and reduce stress on other generation units. Throughout the daytime (10:00–18:00), BT's charging/discharging is dynamically adjusted based on real-time load and generation: discharging during high demand and charging during surplus generation to maintain grid balance. During the evening peak (18:00–22:00), BT discharges again to provide additional

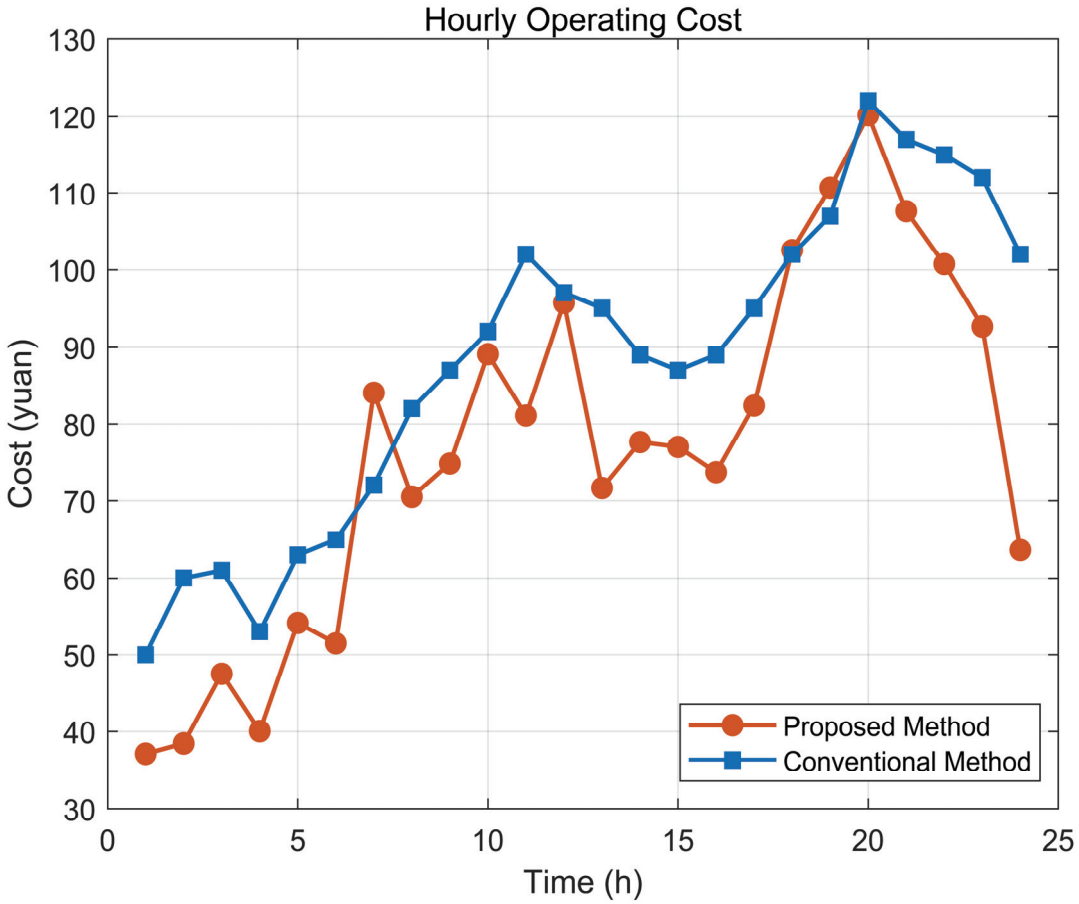

Fig. 4. Comparison of operating costs.

power support. At night (22:00–24:00), as load decreases, BT re-enters charging mode to prepare for the next cycle. This charging/discharging cycle smooths load fluctuations, reduces stress on other power sources, and enhances microgrid stability and reliability, acting as a smart energy regulator in optimal dispatch strategies.

In islanded microgrid operations, components like MT, FC, X, and BT collaboratively operate to maintain power stability: MT and FC adjust output dynamically across load cycles, X manages demand flexibility, and BT balances energy through storage/retrieval, collectively ensuring reliable, efficient, and adaptable microgrid performance.

When the microgrid system is in islanded operation, the costs generated by different scheduling strategies are different. To enhance the economic responsiveness of scheduling, a time-of-use (TOU) pricing mechanism is introduced to differentiate the value of electric energy across different time periods. Combining the regional load level and intraday price fluctuations, the TOU pricing is shown in TABLE 1.

TABLE I
TIME-OF-USE (TOU) PRICING

time period	tariff category	electricity price (CNY/kWh)
00:00-06:00	Low	0.35
06:00-10:00	High	0.85
10:00-17:00	Intermediate	0.55
17:00-21:00	High	0.85
21:00-00:00	Intermediate	0.55

Fig. 4 is a comparison chart of the operating costs of the microgrid using the conventional scheduling strategy and the time-of-use scheduling strategy.

By analyzing the curves in Fig.4, it can be seen that between 6:00 and 8:00 and between 18:00 and 19:00, which are the peak periods of load electricity consumption, the cost of the optimized scheduling strategy using the improved ant colony algorithm in the microgrid is slightly higher than that of the conventional scheduling strategy. When the power of the microgrid cannot meet the electricity demand of the load, the gas turbine starts to be used, and starting the gas turbine will increase the corresponding cost. Therefore, during these time periods, the conventional scheduling method can be adopted for optimized scheduling to minimize the total cost. Overall, the total cost of the microgrid optimized scheduling using the improved ant colony algorithm is lower than that of the conventional algorithm, which verifies the effectiveness and feasibility of the algorithm.

VI. CONCLUSIONS

To solve the problems of slow convergence speed and local optimality that are prone to occur in traditional microgrid scheduling strategies, this paper proposes a microgrid optimized scheduling strategy based on the improved ant colony algorithm. Through simulation and case study analysis, the following conclusions are obtained.

(1) By incorporating regulation factor decay parameters, Boltzmann selection strategy, and other enhancements, the improved algorithm expands the search space, avoids local optima traps, accelerates convergence speed, and generates optimized solution sets closer to the true optimal solution.

(2) The given scheduling strategy effectively reduces microgrid operational costs. Through rational coordination of generation units and prioritized utilization of clean energy sources, it simultaneously decreases power generation expenses and pollutant emissions, and achieves dual objectives of economic enhancement and environmental friendliness.

(3) The optimized algorithm improves the management of energy storage systems and sheddable loads. The energy storage system implements peak shaving and valley filling to alleviate stress on generation equipment, while sheddable loads ensure power supply to critical loads. Their synergistic operation significantly improves microgrid stability and reliability under complex scenarios such as islanded operation.

REFERENCES

[1] W. Zhang, Q. Zhu and H. Zheng, "Economic and optimal dispatch model of electricity, heat and gas for virtual power plants in parks considering low carbon targets," *Engineering Letters*, vol.31, no.1, pp.93-104, 2023.

[2] C. Liu, J. Zhuo, D. Zhao, S. Li, J. Chen, J. Wang and Q. Yao, "Review on flexible and secure operation of renewable energy microgrids using energy storage systems," *Proceedings of the CSEE*, vol.40, no.1, pp.1-18, 2020.

[3] Y. Wang, Y. Cai, Z. Chang, Y. Shang, F. Gao and Q. Sun, "An optimal dispatching algorithm of microgrid based on improved particle filter," *IAENG International Journal of Applied Mathematics*, vol.54, no.10, pp.2099-2107, 2024.

[4] X. Du, S. Zhao, J. Wang and A. He, "Design of double decoupled phase-locked loop of microgrid and smooth switching control strategy for on-grid and off-grid connection," *IAENG International Journal of Computer Science*, vol. 48, no.2, pp.392-405, 2021.

[5] Z. Lei, Q. Xu, G. Hao, C. Wei and M. Yang, "Voltage coordination control strategy for low voltage distribution networks in western rural areas under photovoltaic storage access," *Engineering Letters*, vol.32, no.7, pp.1412-1423, 2024.

[6] S. Zhao, J. Wang, H. Wang and A. He, "Control strategies of microgrid at micro-source level and system level," *Engineering Letters*, vol. 28, no.1, pp.155-167, 2020.

[7] Y. Xing and T. Ren, "Application research of improved MOPSO in optimal scheduling of microgrids," *Acta Energiae Solaris Sinica*, vol.45, no.6, pp.191-200, 2024.

[8] B. Sun, G. Zhao, J. Li and Z. Zhao, "Research on multi-objective optimal scheduling of microgrid based on improved bird swarm algorithm," *Smart Power*, vol.52, no.6, pp.46-53, 99, 2024.

[9] W. Li, Z. Peng, H. Zhang, M. Zhang and H. Fang, "Optimal method for power supply capacity of island-reef hybrid power generation system based on adaptive ant colony algorithm," *Chinese Journal of Ship Research*, vol.19, no.4, pp. 139-147, 2024.

[10] X. Li, D. Li, Z. Zhang, X. Qin, Z. Hong, W. Hu, C. Zhang and Z. Zhang, "Hybrid control strategy and dynamic filtering technology for islanded microgrid systems," *Global Energy Interconnection*, vol.7, no.3, pp.336-347, 2024.

[11] X. Liu, Y. Zhang and X. Liu, "Capacity configuration of hybrid energy storage in microgrid based on ICEEMDAN," *Southern Power System Technology*, vol.19, no.1, pp.140-149, 2025.

[12] Z. Wang, Z. Dou, J. Dong, S. Si, C. Wang and L. Liu, "Optimal dispatching of regional interconnection multi-microgrids based on multi-strategy improved whale optimization algorithm," *IEEJ Transactions on Electrical and Electronic Engineering*, vol.17, no.6, pp. 766-779, 2022.

[13] A. Thaiban, A. Elmitwally, A. Ghanem and I. Omar, "Power quality enhancement based disturbance rejection controller in microgrid system using walrus optimization algorithm and multi-functional recurrent fuzzy neural network," *Ain Shams Engineering Journal*, vol.16, no.9, pp.103540, 2025.

[14] H. Zhou, Y. Zhang, L. Xiao and G. Zhao, "Economic optimal scheduling of microgrid clusters using an improved vulture algorithm," *Acta Energiae Solaris Sinica*, vol.45, no.2, pp.328-335, 2024.

[15] F. Li, X. Wei, Y. Chen, G. Guo and J. Zhang, "Optimal scheduling of microgrids using an improved cuckoo algorithm," *Control Engineering*, vol.31, no.11, pp.1963-1971, 2024.

[16] Y. Xu and H. Wang, "Optimal scheduling of microgrids using an improved grey wolf algorithm," *Computer Simulation*, vol.40, no.3, pp.96-102, 2023.

[17] G. Chen, X. Wang, S. Mo, J. Zhang, W. Xiong, H. Long and M. Zou, "Multi-objective power flow optimization based on improved hybrid crow search algorithm: a novel approach," *Engineering Letters*, vol.30, no.4, pp.1417-1435, 2022.

[18] G. Xie, M. Zhang, M. Yang and D. Wang, "Economic dispatch of isolated microgrids based on enhanced sparrow search algorithm," *Engineering Letters*, vol.32, no.4, pp.753-760, 2024.